

# Nonreciprocal Landau-Zener tunneling

Sota Kitamura,<sup>1</sup> Naoto Nagaosa,<sup>1,2</sup> and Takahiro Morimoto<sup>1</sup>

<sup>1</sup>*Department of Applied Physics, The University of Tokyo, Hongo, Tokyo, 113-8656, Japan*

<sup>2</sup>*RIKEN Center for Emergent Matter Sciences (CEMS), Wako, Saitama, 351-0198, Japan*

(Dated: August 5, 2019)

We theoretically study Landau-Zener tunneling in noncentrosymmetric systems, i.e., the crystals without spatial inversion symmetry. A generalized Landau-Zener formula has been derived taking into account the geometric nature of the wavefunctions. The obtained formula shows that nonreciprocal tunneling probability originates from the difference in the Berry connections of the Bloch wavefunctions across the band gap, i.e., shift vector. We also discuss application of our formula to tunneling in a one-dimensional model of a ferroelectrics.

*Introduction.* — Tunneling phenomenon is one of the most remarkable and unique consequences of the wave nature of particles in quantum mechanics, where a particle can penetrate through classically forbidden regions. In solids, the quantum mechanical wavefunctions of electrons form the band structure separated by the energy gaps, and the tunneling can occur between these bands when an electric field is applied. This is called Zener tunneling through the energy gap and has been actively studied [1–10]. A concise formula, i.e., Landau-Zener formula [1, 2], has been obtained for a model Hamiltonian describing the two-band system as

$$H = \begin{pmatrix} \nu k & \delta \\ \delta & -\nu k \end{pmatrix}, \quad (1)$$

where  $\pm\nu k$  are the energy dispersions and  $2\delta$  is the energy gap. Under an external electric field  $E$ , the wavenumber  $k$  is accelerated as  $\dot{k} = -eE$  as shown in Fig. 1(a). The transition probability from the lower band to the upper band reads

$$P = \exp\left(-\frac{\pi\delta^2}{e\hbar E\nu}\right), \quad (2)$$

which is essentially singular with respect to  $E$  showing the nonperturbative nature of the quantum tunneling. (Hereafter we set  $\hbar = 1$  for simplicity.)

At a pn-junction of semiconductors, the tunneling shows an asymmetric behavior, which is utilized as a tunneling diode for rectifying devices [11]. Because of the broken inversion symmetry, the tunneling probability, and hence, the I-V characteristics depend strongly on the direction of the electric field  $E$ . For the uniform bulk crystal, however, the asymmetry in the Zener tunneling probability is a highly nontrivial issue even when the crystal lacks the inversion symmetry. This can be seen in the band dispersion  $\varepsilon_n(k)$  ( $n$ : band index); the relation  $\varepsilon_n(k) = \varepsilon_n(-k)$  holds due to the time-reversal symmetry even in the absence of the spatial inversion symmetry. Therefore, the inversion symmetry is rather hidden in wave mechanics [12]. Intuitively, the extended wave state is rather insensitive to the broken inversion symmetry compared with the localized wave-packet. Therefore, a fundamental question is how the nonreciprocal behavior, i.e., the asymmetry between the opposite direction of the electric field  $E$ , is realized in the tunneling processes of the bulk crystals, reflecting the wave nature of the electrons.

The nonreciprocal phenomena in noncentrosymmetric crystals have been extensively studied in these days, including both the dc transport [13–18] and photo-excited current [19–26]. In particular, the NO-GO theorem has been proposed for the nonreciprocal transport of independent particles induced by the static electric field, in terms of a perturbative expansion with respect to  $E$  [27]. Instead, the interacting electrons can show nonreciprocal dc transport in a perturbative treatment. On the other hand, this theorem does not apply for the photocurrent induced by the light irradiation which induces the inter-band transitions, which is called shift current. The shift current is formulated in terms of the Berry connection of the Bloch wavefunctions, which correspond to the intracell coordinates of the electrons [23–26, 28]. The optical transition causes the shift in the intracell coordinates, i.e., shift vector, since intracell coordinates are generally different for the valence and conduction bands in noncentrosymmetric crystals. The steady pumping of polarization of photoexcited electron-hole pairs results in the dc photocurrent. Therefore, it is concluded that the wavefunctions encode the information of the noncentrosymmetry in sharp contrast to the energy dispersion. In fact, the Berry phase becomes zero (or trivial) when the system preserves both the inversion and time-reversal symmetries.

As discussed above, the tunneling is a nonperturbative effect, and cannot be captured by the perturbative expansion with respect to  $E$ . Hence, it is possible that the nonreciprocal nature appears in the Landau-Zener tunneling even in the independent particle approximation. Indeed, we show below that this is the case by deriving the generalized Landau-Zener formula including the shift vector, i.e., the information of the Bloch wavefunctions.

*Tunneling formula with a shift vector.* — Let us consider a time evolution of a system under a slow change of parameters. In particular, here we focus on a change of momentum  $k$  under a DC electric field,  $k \rightarrow k(t) = k - eEt$  (We set  $e = 1$  hereafter, for simplicity). It is well known that the solution of the time-dependent Schrödinger equation in the adiabatic limit is given by snapshot eigenstates

$$H(t)|n, k(t)\rangle = \varepsilon_n(t)|n, k(t)\rangle \quad (3)$$

multiplied by dynamical and Berry phase factors. The diabatic correction is derived from the transition dipole matrix

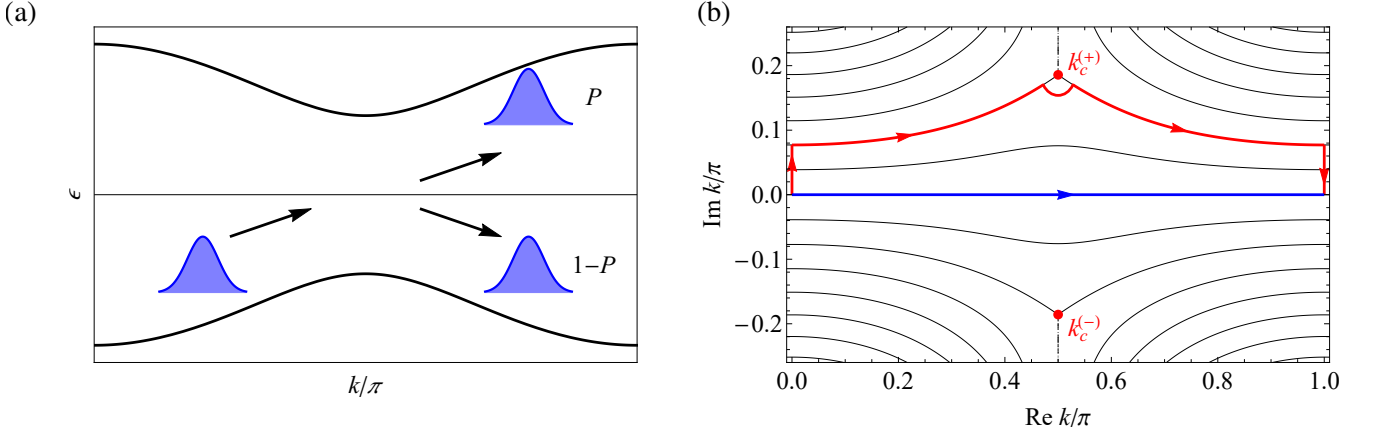


FIG. 1. (a) Schematics of Landau-Zener tunneling. A wave packet driven by an electric field can tunnel into the conduction band with transition probability  $P$ . (b) Complex  $k$  plane that governs the tunneling process. The branching point  $k_c$  is a point where the band gap vanishes in the complex plane. Cauchy's theorem allows to deform the original integration path on the real axis (blue) into the contour in the complex plane that passes through the branching point (red).

elements. To see this, let us expand a state vector  $|\Psi\rangle$  by the adiabatic solutions as

$$|\Psi\rangle = \sum_n a_n(t) e^{-i \int_0^t dt_1 [\varepsilon_n(t_1) + EA_{nn}(t_1)]} |n, k(t)\rangle, \quad (4)$$

where  $A_{nm}(t) = i\langle n, k(t) | \partial_k | m, k(t) \rangle$  is the Berry connection. (We note that the ‘‘off-diagonal’’ Berry connections for  $n \neq m$  correspond to transition dipole matrix elements.) With paying attention in dealing with the Berry phase factor, we can reduce the time-dependent Schrödinger equation  $i\partial_t |\Psi\rangle = H(t) |\Psi\rangle$  to [29]

$$i\partial_t a_n(t) = E \sum_{m \neq n} |A_{nm}(t)| e^{i \int_0^t dt_1 [\varepsilon_n - \varepsilon_m - ER_{nm}] + i \arg A_{nm}(t_0)} a_m(t), \quad (5)$$

with

$$R_{nm} = -A_{nm} + A_{mm} + \partial_k \arg A_{nm}. \quad (6)$$

Here we have used  $\partial_t = -E\partial_k$  for  $|n, k(t)\rangle$  and  $\arg A_{nm}(t)$ .  $R_{nm}$  is nothing but the shift vector, which is a gauge-invariant object describing the polarization difference between two bands  $n, m$ . This fact is usually overlooked when  $A_{nm} = 0$  is assumed.

Let us focus on a tunneling process between two bands,  $n = \pm$  with  $a_-(t_0) = 1$ ,  $a_+(t_0) = 0$ . Our goal is to derive the tunneling rate  $P = |a_+(t)|^2$  after one cycle of the Bloch oscillation. For simplicity, we consider only the first-order correction w.r.t.  $|A_{+-}|$  here. By integrating Eq. (5) and using it recursively, we obtain [29]

$$a_+(t) = i e^{i \arg A_{+-}(t_0)} \times \int_{k_0}^{k_0 - Et} dk_1 |A_{+-}| \exp \left[ -i \int_{k_0}^{k_1} dk_2 \left( \frac{\varepsilon_+ - \varepsilon_-}{E} - R_{+-} \right) \right]. \quad (7)$$

A two-band Hamiltonian can be represented as  $H = \mathbf{d}(k) \cdot \boldsymbol{\sigma}$  with  $\boldsymbol{\sigma}$  being Pauli matrices (when we subtract a constant

energy shift). The quantities necessary for the evaluation of the tunneling amplitude are given as

$$\varepsilon_+ - \varepsilon_- = 2\sqrt{\mathbf{d}^2}, \quad (8)$$

$$|A_{+-}| = \frac{\sqrt{(\partial_k \mathbf{d} \times \mathbf{d})^2}}{2\mathbf{d}^2}, \quad (9)$$

$$R_{+-} = -\frac{(\partial_k \mathbf{d} \times \mathbf{d}) \cdot (\partial_k^2 \mathbf{d})}{(\partial_k \mathbf{d} \times \mathbf{d})^2} \sqrt{\mathbf{d}^2}. \quad (10)$$

In order to evaluate the integral in an asymptotic manner, we employ the Dykhne-Davis-Pechukas (DDP) method [3, 4] in accordance with Ref. 3. Namely, we perform the integral by means of contour integration in the complex plane. The contour of the integral, which is originally the real axis [blue line in Fig. 1(b)], can be deformed within an analytic region, thanks to the Cauchy's integral theorem.

This treatment is advantageous since one can utilize a (complex) branching point  $k_c$  where the energy gap vanishes  $\mathbf{d}(k_c)^2 = 0$  [Such a point is indeed a branching point when the Hamiltonian is analytic, as  $\varepsilon_+ - \varepsilon_- \propto (k - k_c)^{1/2}$  in the vicinity of  $k_c$ ]. This point essentially governs the tunneling process between the two bands: Since the prefactor  $|A_{+-}|$  diverges as we approach  $k_c$  [see Eq. (9)], only this divergent part contributes to the asymptotic value of the integral, when the integration path is deformed to pass through the vicinity of the branching point  $k_c$ .

We show the integration path by a red line in Fig. 1(b). The main part of the contour is one along which the absolute value of the exponential factor is constant (i.e., the imaginary part of the  $k_2$  integral in Eq. (7) is constant). This contour passes through the branching point  $k_c$ , but we make a detour around it since  $k_c$  itself is a singular point of the integrand. Due to the divergence mentioned above, this detoured part contributes dominantly against the main part. The integral on the first and last vertical lines cancel each other due to the periodicity. While the branching points appear in a pairwise manner

$(k_c, k_c^*)$ , we choose one of them such that the exponential factor becomes smaller than unity.

In a generic situation, one can assume that the leading order term of  $\mathbf{d}^2$ ,  $(\partial_k \mathbf{d})^2$  and  $(\partial_k \mathbf{d} \times \mathbf{d}) \cdot (\partial_k^2 \mathbf{d})$  in the expansion around  $k_c$  is given as  $\mathbf{d}^2 \sim i\alpha(k - k_c)$ ,  $(\partial_k \mathbf{d})^2 \sim \beta$ , and  $(\partial_k \mathbf{d} \times \mathbf{d}) \cdot (\partial_k^2 \mathbf{d}) \sim \eta$ , respectively. By evaluating the detoured part of the integral [circular arc around  $k_c$  in Fig. 1(b)] with these expanded forms, we arrive at

$$P \sim \exp \left[ 2\text{Im} \int_{k_0}^{k_c} dk_2 \left( \frac{\varepsilon_+ - \varepsilon_-}{E} - R_{+-} \right) \right], \quad (11)$$

as we describe in Supplementary Materials [29]. Note that, there is a prefactor  $(\pi/3)^2 \sim 1.1$  in the actual calculation, but here we drop it because the prefactor is exactly unity if we evaluate the full solution of Eq. (5) in the same way [3].

The obtained formula, Eq. (11), includes the geometric correction described by the shift vector. This contribution is absent in the original DDP formula, because they assumed that the  $2 \times 2$  Hamiltonian is real; Under this assumption  $\mathbf{d}$  is a two-dimensional vector, where  $(\partial_k \mathbf{d} \times \mathbf{d}) \cdot (\partial_k^2 \mathbf{d}) = 0$  always holds. On the other hand, Refs. 6 and 7 dealt with a generic  $2 \times 2$  Hamiltonian, so that the geometric correction indeed appeared in their study. However, their calculation was done in a particular gauge, and the obtained expression is not gauge-invariant. Comparison of the formula is given in the Supplementary Materials [29]. Our result is expressed in terms of gauge-invariant quantities, the shift vector, so that it provides much clearer understanding on the physical interpretation of the correction and remarkable physical consequences due to it.

The shift vector  $R_{nm}$  plays a crucial role in the nonlinear transport of inversion-broken systems. It satisfies  $R_{nm}(k) = -R_{nm}(-k)$  when the system is time-reversal symmetric, while  $R_{nm}(k) = R_{nm}(-k)$  when the system is inversion symmetric. Thus when the system has both symmetries, there is no correction to the tunneling probability; This is consistent with the fact that one can make the Hamiltonian real in such cases. A nontrivial result thus can appear when either symmetry is broken. In particular, a qualitatively new phenomenon appears when the inversion symmetry is broken: When we change the sign of the electric field  $E$ , we need to change the choice of the branching point from  $k_c$  to  $-k_c$  in order to have a correct result  $P \leq 1$  with the formula (11). Under this alternation, the

shift vector contribution is invariant in the time-reversal broken system, which leads to a simple correction of the probability independent of the field strength/direction. On the other hand, when the inversion symmetry is broken, the exponent of the shift vector correction is odd under this alternation, so that it leads to an exponentially-large difference in the tunneling probability when the direction of the electric field is reverted.

The physical meaning of the shift vector as an intracell coordinate provides an intuitive understanding of its role in the tunneling process, as follows. The tunneling process can be interpreted as a propagation of a wave packet thorough a classically forbidden region in real space, which has a thickness of  $2\delta/E$  as drawn in Fig. 2. Now the noncentrosymmetric system has an internal degree of freedom, the intracell coordinate, whose difference between two bands is represented by the shift vector [See Fig. 2(a)]. Thus the electrons must move an additional distance of  $R$  when the tunneling from the lower band to the upper band occurs. Since the direction of the shift vector is intrinsically determined by the underlying crystal, this additional distance contributes in a constructive/destructive manner in accordance with the direction of the bias, as shown in Figs. 2(b) and (c).

*Application to Rice-Mele model.* — Let us see the emergence of the nonreciprocal (direction-dependent) tunneling probability using the Rice-Mele model

$$H = \begin{pmatrix} m & t \cos k - i\delta t \sin k \\ t \cos k + i\delta t \sin k & -m \end{pmatrix}, \quad (12)$$

a prototypical example of an inversion-broken (polar) system. Indeed, this model has a finite shift vector

$$R_{+-} = \frac{m t \delta t \sqrt{t^2 \cos^2 k + \delta t^2 \sin^2 k + m^2}}{m^2 (\delta t^2 \cos^2 k + t^2 \sin^2 k) + t^2 \delta t^2}. \quad (13)$$

Since the integrand of Eq. (11) for the present system is invariant under  $k \rightarrow k \pm \pi$ , let us consider a slow parameter change  $k : 0 \rightarrow -\pi \text{sgn}(E)$ . The branching point of the present model is given as

$$k_c^{(\pm)} = \frac{2n+1}{2} \pi \pm i \tanh^{-1} \sqrt{\frac{\delta t^2 + m^2}{t^2 + m^2}} \quad (14)$$

with  $n \in \mathbb{Z}$ . By evaluating the generalized formula (11) with  $k_c = k_c^{(-\text{sgn}(E))}$ , we obtain

$$P = \exp \left[ -\frac{4 \sqrt{t^2 + m^2}}{|E|} (K(\gamma) - E(\gamma)) + \frac{2m \text{sgn}(E)}{t \delta t \sqrt{t^2 + m^2}} \left( t^2 K(\gamma) - (t^2 - \delta t^2) \Pi \left( \frac{\delta t^2}{t^2}, \gamma \right) \right) \right] \quad (15)$$

$$\sim \exp \left[ -\frac{\pi(\delta t^2 + m^2)}{|E|t} + \text{sgn}(E) \frac{\pi m \delta t}{2t^2} \right] \quad (\delta t, m \ll t), \quad (16)$$

where  $K(\gamma)$ ,  $E(\gamma)$ , and  $\Pi(n, \gamma)$  are the complete elliptic inte-

grals with  $\gamma = \sqrt{(\delta t^2 + m^2)/(t^2 + m^2)}$  being the elliptic mod-

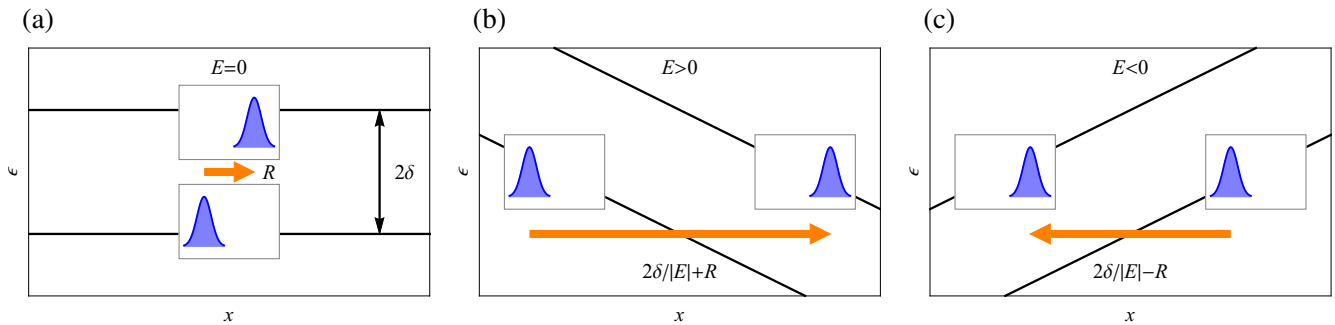


FIG. 2. Zener tunneling in inversion broken systems. (a) Real space picture in the absence of the electric field  $E$ . The positions of the wave packets in the two bands are shifted in the unit cell by the shift vector  $R$ . (b,c) Real space pictures of two bands in the presence of  $E$ . The shift in the intracell coordinate results in the different tunneling depth depending on the direction of  $E$  by the shift vector  $R$ .

ulus. In the last line, we recover the conventional exponent Eq. (2) for the  $|E|^{-1}$  term ( $\delta \rightarrow \sqrt{\delta t^2 + m^2}$  and  $v \rightarrow t$ ). The shift vector correction is represented as  $\text{sgn}(E) \times (\pi\delta/2v) \times R_{+-}$  evaluated at  $k = \pi/2$ . Remarkably, as we have mentioned, the non-zero shift vector not just provides an exponentially-large correction, but also a strong nonreciprocity via  $\text{sgn}(E)$ .

Using the obtained generalized Landau-Zener formula, we show the tunneling probability  $P$  in Rice-Mele model in Fig. 3. Plots of  $P(E)$  as a function of the applied electric field  $E$  (Fig. 3(a)) show a well-known nonperturbative behavior at  $E = 0$  and a good agreement with tunneling rates obtained by numerically solving time-dependent Schrödinger equation (shown in dots). In addition, they show that tunneling probabilities differ depending on the direction of  $E$  (the sign of  $E$ ). This direction dependence arises from the nonzero shift vector and shows almost proportionality to the value of  $R_{+-}$  at the band gap minimum (on the real axis of  $k$ ). Figure 3(b) shows the nonreciprocity ratio  $P(+E)/P(-E)$  (the ratio of tunneling probabilities for positive and negative  $E$ ) which quantifies the strength of nonreciprocity as a rectifying device. The ratio  $P(+E)/P(-E)$  grows monotonically, as a function of the strength of alternating hopping  $\delta t$  that introduces inversion symmetry breaking. For small  $\delta t$ , the nonreciprocity ratio is linearly proportional to  $\delta t$ . In particular, large nonreciprocity of  $P(+E)/P(-E) \sim 2$  can be achieved for a feasible value of  $\delta t \sim 0.5t$ , which indicates that Landau Zener tunneling in noncentrosymmetric crystals is able to realize strong nonreciprocal functionality.

*Discussions.* — Here we further consider the role of time-reversal symmetry  $T$  in the nonreciprocal responses. In the context of magnetochiral anisotropy [13–17], it has been discussed that the nonreciprocal transport requires the broken  $T$  in addition to the broken inversion symmetry. This can be understood intuitively that the reversal of time corresponds to that of the current direction when there is no dissipation. The NO-GO theorem in Ref. 27 indeed shows that the current proportional to the square of the electric field is forbidden in non-interaction systems with dc electric field, when the  $T$ -symmetry is preserved. However, it has been revealed that this is not the case when the inter-band transitions and the as-

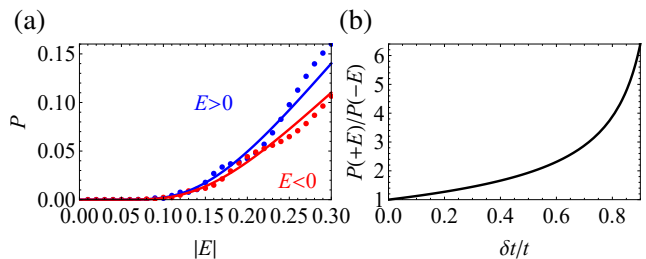


FIG. 3. (a) Nonreciprocal tunneling probability  $P(E)$  in Rice-Mele model. Solid lines represent  $P(E)$  from the generalized Landau-Zener formula, and dots represent  $P(E)$  obtained from numerical simulations of time-dependent Schrödinger equation. We used the parameters  $(\delta t, m) = (0.2t, 0.4t)$ . (b) Nonreciprocity ratio  $P(+E)/P(-E)$  plotted as a function of alternating hopping amplitude  $\delta t$  that controls the magnitude of inversion breaking. We set  $m = 0.4t$ .

sociated absorption of energy occur due to ac  $E$ -field, where the shift current is induced. The Zener tunneling studied in the present paper can be regarded as the “inter-band” transition under dc  $E$ -field due to the tunneling, and hence the NO-GO theorem, which is based on the adiabatic assumption that there occurs no inter-band transition, does not apply. This is related to the non-analytic and non-perturbative nature of the tunneling probability, which cannot be expanded in  $E$ . In a more general situation in the plane of the frequency  $\omega$  and the strength  $E$  of the electric field, there are several different regions as indicated by Fig. 17 of Ref. 30. In this respect, the shift current and Zener tunneling are two limiting cases, i.e., ac limit of weak  $E$ -field and dc limit of strong  $E$ -field, and the crossover between these two corresponds to the Keldysh line and how the nonreciprocal responses behaves in this plane is an interesting problem to be studied in the future. Note that from the viewpoint of the symmetry, the requirement for the nonreciprocal Zener tunneling is the same as that for the shift current. Another unique feature of the nonreciprocal Zener tunneling is that the ratio of the tunneling currents for the two directions is independent of the electric field  $E$  and is of the order of unity as indicated in Eq. (16).

In the present paper, we considered the spinless model. In-

corporating the spin degrees of freedom and spin-orbit interaction, one can expect the nonreciprocal charge and spin tunneling currents. These phenomena can offer novel mechanisms for spin diode or switchable diode by a magnetic field. The large spin polarization of the electrons transmitted through the DNA molecules that has been observed experimentally [31] might be understood from this point of view [32].

*Acknowledgments.* — This work was supported by The University of Tokyo Excellent Young Researcher Program (TM), JST CREST Grant (JPMJCR1874 and JPMJCR16F1) and JSPS KAKENHI (18H03676 and 26103006)(NN).

- 
- [1] L. Landau and E. Lifshitz, *Quantum Mechanics: Non-Relativistic Theory*, Course of Theoretical Physics (Elsevier Science, 1981).
- [2] C. Zener, “Non-adiabatic crossing of energy levels,” *Proceedings of the Royal Society of London. Series A*, **137**, 696 (1932).
- [3] J. P. Davis and P. Pechukas, “Nonadiabatic transitions induced by a time-dependent Hamiltonian in the semiclassical/adiabatic limit: The two-state case,” *J. Chem. Phys.* **64**, 3129 (1976).
- [4] A. Dykhne, “Adiabatic perturbation of discrete spectrum states,” *Sov. Phys. JETP* **14**, 1 (1962).
- [5] T. F. George and Y.-W. Lin, “Multiple transition points in a semiclassical treatment of electronic transitions in atom/ion-diatom collisions,” *J. Chem. Phys.* **60**, 2340 (1974).
- [6] A. Joye, H. Kunz, and C.-E. Pfister, “Exponential decay and geometric aspect of transition probabilities in the adiabatic limit,” *Annals of Physics* **208**, 299 (1991).
- [7] A. Joye, G. Miletì, and C.-E. Pfister, “Interferences in adiabatic transition probabilities mediated by Stokes lines,” *Phys. Rev. A* **44**, 4280 (1991).
- [8] K. Saito, M. Wubs, S. Kohler, Y. Kayanuma, and P. Hänggi, “Dissipative Landau-Zener transitions of a qubit: Bath-specific and universal behavior,” *Phys. Rev. B* **75**, 214308 (2007).
- [9] Y. Kayanuma and K. Saito, “Coherent destruction of tunneling, dynamic localization, and the Landau-Zener formula,” *Phys. Rev. A* **77**, 010101 (2008).
- [10] T. Oka, “Nonlinear doublon production in a Mott insulator: Landau-Dykhne method applied to an integrable model,” *Phys. Rev. B* **86**, 075148 (2012).
- [11] L. Esaki, “New Phenomenon in Narrow Germanium  $p-n$  Junctions,” *Phys. Rev.* **109**, 603 (1958).
- [12] Y. Tokura and N. Nagaosa, “Nonreciprocal responses from noncentrosymmetric quantum materials,” *Nat. Commun.* **9**, 3740 (2018).
- [13] G. L. J. A. Rikken, J. Fölling, and P. Wyder, “Electrical Magnetochiral Anisotropy,” *Phys. Rev. Lett.* **87**, 236602 (2001).
- [14] V. Krstić, S. Roth, M. Burghard, K. Kern, and G. L. J. A. Rikken, “Magneto-chiral anisotropy in charge transport through single-walled carbon nanotubes,” *J. Chem. Phys.* **117** (2002).
- [15] G. Rikken and E. Raupach, “Observation of magneto-chiral dichroism,” *Nature* **390**, 493 (1997).
- [16] G. L. J. A. Rikken and P. Wyder, “Magnetolectric Anisotropy in Diffusive Transport,” *Phys. Rev. Lett.* **94**, 016601 (2005).
- [17] F. Pop, P. Auban-Senzier, E. Canadell, G. L. Rikken, and N. Avarvari, “Electrical magnetochiral anisotropy in a bulk chiral molecular conductor,” *Nat. Commun.* **5**, 3757 (2014).
- [18] R. Wakatsuki, Y. Saito, S. Hoshino, Y. M. Itahashi, T. Ideue, M. Ezawa, Y. Iwasa, and N. Nagaosa, “Nonreciprocal charge transport in noncentrosymmetric superconductors,” *Sci. Adv.* **3**, e1602390 (2017).
- [19] I. Grinberg, D. V. West, M. Torres, G. Gou, D. M. Stein, L. Wu, G. Chen, E. M. Gallo, A. R. Akbashev, P. K. Davies, *et al.*, “Perovskite oxides for visible-light-absorbing ferroelectric and photovoltaic materials,” *Nature* **503**, 509 (2013).
- [20] W. Nie, H. Tsai, R. Asadpour, J.-C. Blancon, A. J. Neukirch, G. Gupta, J. J. Crochet, M. Chhowalla, S. Tretiak, M. A. Alam, H.-L. Wang, and A. D. Mohite, “High-efficiency solution-processed perovskite solar cells with millimeter-scale grains,” *Science* **347**, 522 (2015).
- [21] D. Shi, V. Adinolfi, R. Comin, M. Yuan, E. Alarousu, A. Buin, Y. Chen, S. Hoogland, A. Rothenberger, K. Katsiev, Y. Losovyj, X. Zhang, P. A. Dowben, O. F. Mohammed, E. H. Sargent, and O. M. Bakr, “Low trap-state density and long carrier diffusion in organolead trihalide perovskite single crystals,” *Science* **347**, 519 (2015).
- [22] D. W. de Quilettes, S. M. Vorpahl, S. D. Stranks, H. Nagaoka, G. E. Eperon, M. E. Ziffer, H. J. Snaith, and D. S. Ginger, “Impact of microstructure on local carrier lifetime in perovskite solar cells,” *Science* **348**, 683 (2015).
- [23] J. E. Sipe and A. I. Shkrebtii, “Second-order optical response in semiconductors,” *Phys. Rev. B* **61**, 5337 (2000).
- [24] S. M. Young and A. M. Rappe, “First Principles Calculation of the Shift Current Photovoltaic Effect in Ferroelectrics,” *Phys. Rev. Lett.* **109**, 116601 (2012).
- [25] A. M. Cook, B. M. Fregoso, F. de Juan, S. Coh, and J. E. Moore, “Design principles for shift current photovoltaics,” *Nat. Commun.* **8**, 14176 (2017).
- [26] T. Morimoto and N. Nagaosa, “Topological nature of nonlinear optical effects in solids,” *Sci. Adv.* **2**, e1501524 (2016).
- [27] T. Morimoto and N. Nagaosa, “Nonreciprocal current from electron interactions in noncentrosymmetric crystals: roles of time reversal symmetry and dissipation,” *Sci. Rep.* **8**, 2973 (2018).
- [28] N. Nagaosa and T. Morimoto, “Concept of Quantum Geometry in Optoelectronic Processes in Solids: Application to Solar Cells,” *Advanced Materials* **29**, 1603345 (2017).
- [29] See Supplemental Material attached below for further details.
- [30] H. Aoki, N. Tsuji, M. Eckstein, M. Kollar, T. Oka, and P. Werner, “Nonequilibrium dynamical mean-field theory and its applications,” *Rev. Mod. Phys.* **86**, 779 (2014).
- [31] B. Göhler, V. Hamelbeck, T. Z. Markus, M. Kettner, G. F. Hanne, Z. Vager, R. Naaman, and H. Zacharias, “Spin Selectivity in Electron Transmission Through Self-Assembled Monolayers of Double-Stranded DNA,” *Science* **331**, 894 (2011).
- [32] S. Matityahu, Y. Utsumi, A. Aharony, O. Entin-Wohlman, and C. A. Balseiro, “Spin-dependent transport through a chiral molecule in the presence of spin-orbit interaction and nonunitary effects,” *Phys. Rev. B* **93**, 075407 (2016).

## Supplemental Material

### Derivation of Eqs. (5, 7)

Here we provide a detailed derivation of Eqs. (5, 7) in the main text. By inserting Eq. (4) to the time-dependent Schrödinger equation, we obtain

$$\sum_m e^{-i \int_0^t dt_1 [\varepsilon_m(t_1) + EA_{mm}(t_1)]} \{ [i\partial_t a_m(t) + Ea_m(t)A_{mm}(t)] |m, k(t)\rangle - Ea_m(t) i\partial_k |m, k(t)\rangle \} = 0. \quad (S1)$$

Here we have used  $\partial_t |m, k(t)\rangle = -E\partial_k |m, k(t)\rangle$ . By taking an inner product with  $\langle n, k(t) |$ ,  $\langle n, k(t) | m, k(t)\rangle = \delta_{nm}$  and  $\langle n, k(t) | i\partial_k |m, k(t)\rangle = A_{nm}(t)$  leads to

$$i\partial_t a_n(t) = E \sum_{m \neq n} A_{nm}(t) e^{i \int_0^t dt_1 [\varepsilon_n(t_1) + EA_{nm}(t_1)]} e^{-i \int_0^t dt_1 [\varepsilon_m(t_1) + EA_{mm}(t_1)]} a_m(t) \quad (S2)$$

$$= E \sum_{m \neq n} |A_{nm}(t)| e^{i \int_0^t dt_1 [\varepsilon_n - \varepsilon_m + E(A_{nn} - A_{mm})] + i \arg A_{nm}(t)} a_m(t) \quad (S3)$$

$$= E \sum_{m \neq n} |A_{nm}(t)| e^{i \int_0^t dt_1 [\varepsilon_n - \varepsilon_m + E(A_{nn} - A_{mm}) + \partial_t \arg A_{nm}] + i \arg A_{nm}(t_0)} a_m(t) \quad (S4)$$

$$= E \sum_{m \neq n} |A_{nm}(t)| e^{i \int_0^t dt_1 [\varepsilon_n - \varepsilon_m + E(A_{nn} - A_{mm}) - \partial_k \arg A_{nm}] + i \arg A_{nm}(t_0)} a_m(t). \quad (S5)$$

This coincides with Eq. (5).

By integrating Eq. (5) from  $t_0$  to  $t$ , we obtain

$$a_n(t) = a_n(t_0) - iE \int_{t_0}^t dt_1 \sum_{m \neq n} |A_{nm}(t_1)| e^{i \int_0^{t_1} dt_2 [\varepsilon_n - \varepsilon_m - ER_{nm}] + i \arg A_{nm}(t_0)} a_m(t_1). \quad (S6)$$

$$\begin{aligned} &= a_n(t_0) - iE \int_{t_0}^t dt_1 \sum_{m \neq n} |A_{nm}(t_1)| e^{i \int_0^{t_1} dt_2 [\varepsilon_n - \varepsilon_m - ER_{nm}] + i \arg A_{nm}(t_0)} a_m(t_0) \\ &\quad + (-iE)^2 \int_{t_0}^t dt_1 \int_{t_0}^{t_1} dt_2 \sum_{m \neq n} \sum_{l \neq m} |A_{nm}(t_1)| |A_{ml}(t_2)| e^{i \int_0^{t_1} dt_2 [\varepsilon_n - \varepsilon_m - ER_{nm}] + i \int_0^{t_2} dt_3 [\varepsilon_m - \varepsilon_l - ER_{ml}] + i \arg A_{nm}(t_0) + i \arg A_{ml}(t_0)} a_l(t_2)}. \end{aligned} \quad (S7)$$

Let us neglect the third term  $O(|A|^2)$  in the last line, and set  $n = +$ ,  $m = -$ .  $a_-(t_0) = 1$  and  $a_+(t_0) = 0$  leads to Eq. (7) as

$$a_+(t) = -iE \int_{t_0}^t dt_1 |A_{+-}(t_1)| e^{i \int_0^{t_1} dt_2 [\varepsilon_+ - \varepsilon_- - ER_{+-}] + i \arg A_{+-}(t_0)} \quad (S8)$$

$$= i \int_{k(t_0)}^{k(t)} dk_1 |A_{+-}(k_1)| e^{-i \int_{k(t_0)}^{k_1} dk_2 \frac{1}{E} [\varepsilon_+ - \varepsilon_- - ER_{+-}] + i \arg A_{+-}(t_0)}. \quad (S9)$$

### Derivation of Eq. (11) with the DDP method

Here we show the detail of the evaluation of Eq. (7) along the deformed contour shown in Fig. 1(b). Let us focus on the detoured part (the circular arc around  $k_c$ ), which yields a dominant contribution. As mentioned in the main text, we assume that  $\mathbf{d}^2 \sim i\alpha(k - k_c)$ ,  $(\partial_k \mathbf{d})^2 \sim \beta$ , and  $(\partial_k \mathbf{d} \times \mathbf{d}) \cdot (\partial_k^2 \mathbf{d}) \sim \eta$  in the vicinity of  $k_c$ . Then  $(\partial_k \mathbf{d} \times \mathbf{d})^2 = (\partial_k \mathbf{d})^2 \mathbf{d}^2 -$

$(\partial_k \mathbf{d}^2)^2 / 4 \sim \alpha^2 / 4$  leads to

$$|A_{+-}| \sim \frac{1}{4i(k - k_c)}, \quad (S10)$$

which, remarkably, does not depend on any detail of the system. We also expand the exponent as

$$\int_{k_0}^{k_1} dk_2 \left( \frac{\varepsilon_+ - \varepsilon_-}{E} - R_{+-} \right) \sim z + \int_{k_0}^{k_c} dk_2 \left( \frac{\varepsilon_+ - \varepsilon_-}{E} - R_{+-} \right), \quad (S11)$$

where

$$z = \frac{4}{3} \sqrt{i\alpha} \left( \frac{1}{E} + \frac{2\eta}{\alpha^2} \right) (k_1 - k_c)^{3/2}. \quad (S12)$$

The main part of the contour (where the absolute value of the exponential factor is constant) extends from  $k_c$  to directions where  $z$  is real. There are three such directions in  $2\pi/3$  intervals, as can be seen in Fig. 1(b). The circular arc connects two of them, so it has an angle  $2\pi/3$ .

Let us choose either  $k_c$  or  $k_c^*$ , such that  $\arg z \in [0, \pi]$  holds on the arc. Then further we set the infinitesimal radius of the arc to be  $\propto |E|^{2/3-\epsilon}$  with  $\epsilon > 0$ . By doing so we can make the contribution of detoured part dominate that of the main part (for rigorous bounds, see Ref. 3. The shift vector correction  $2\eta/\alpha^2$  does not affect the bounds as it is higher-order w.r.t.  $E$ ).

Let us change the integrating variable from  $k_1$  to  $z$ . Then the integral (7) along the detoured contour is given as

$$a_+(t) \sim e^{i \arg A_{+-}(t_0)} \exp \left[ -i \int_{k_0}^{k_c} dk_2 \left( \frac{\varepsilon_+ - \varepsilon_-}{E} - R_{+-} \right) \right] \int_C dz \frac{e^{-iz}}{6z}, \quad (\text{S13})$$

where the contour  $C$  is a semicircle with a radius  $\propto E^{-\epsilon} \rightarrow \infty$  as  $E \rightarrow 0$ , covering the upper half-plane. With the help of the Jordan's lemma, the integral along  $C$  is given by the residue at  $z = 0$ , i.e.,  $\oint dz e^{-iz}/(6z) = i\pi/3$ . Finally we arrive at Eq. (11) multiplied by  $(\pi/3)^2$ . This prefactor should be replaced by unity if we evaluate Eq. (5) in a similar way as

$$\partial_z \begin{pmatrix} a_+(z) \\ \tilde{P}a_-(z) \end{pmatrix} = \frac{1}{6z} \begin{pmatrix} 0 & e^{-iz} \\ e^{iz} & 0 \end{pmatrix} \begin{pmatrix} a_+(z) \\ \tilde{P}a_-(z) \end{pmatrix}, \quad (\text{S14})$$

where  $\tilde{P}$  is the exponential factor in Eq. (S13).

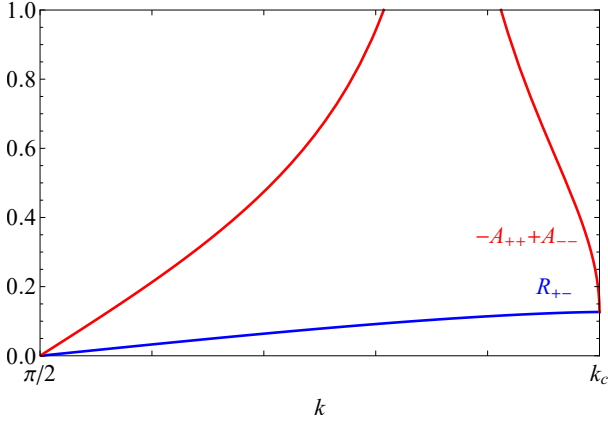


FIG. S1. Comparison of the integral  $\text{Im} \int_{\pi/2}^k dk_2 R_{+-}(k_2)$  with Eq. (10) (blue) and  $\text{Im} \int_{\pi/2}^k dk_2 (-A_{++}(k_2) + A_{--}(k_2))$  with Eq. (S16) (red) for the Rice-Mele model.

## Comparison of Eq. (11) with Ref. 6

Let us evaluate Eq. (11) with eigenvectors

$$|\pm, k(t)\rangle = \frac{(\sqrt{d^2} \pm \mathbf{d} \cdot \mathbf{e}_z) |\uparrow\rangle \pm \mathbf{d} \cdot (\mathbf{e}_x + i\mathbf{e}_y) |\downarrow\rangle}{\sqrt{2(d^2 \pm \sqrt{d^2} \mathbf{d} \cdot \mathbf{e}_z)}}. \quad (\text{S15})$$

For this gauge choice, we obtain

$$-A_{++} + A_{--} = \frac{((\partial_k \mathbf{d} \times \mathbf{d}) \cdot \mathbf{e}_z)(\mathbf{d} \cdot \mathbf{e}_z)}{\sqrt{d^2} (\mathbf{d} \times \mathbf{e}_z)^2}, \quad (\text{S16})$$

$$\arg A_{+-} = \frac{\pi}{2} + \tan^{-1} \frac{2\sqrt{d^2} (\partial_k \mathbf{d} \times \mathbf{d}) \cdot \mathbf{e}_z}{(\mathbf{d} \cdot \mathbf{e}_z) \partial_k d^2 - 2(\partial_k \mathbf{d} \cdot \mathbf{e}_z) d^2}. \quad (\text{S17})$$

If we assume that  $\mathbf{d}(k_c) \cdot \mathbf{e}_z \neq 0$  (in accordance with Ref. [6]),  $\arg A_{+-}(k_c) = \pi/2$  holds in general cases, so that  $\text{Im} \int_{k_0}^{k_c} dk \partial_k \arg A_{+-} = 0$ . Hence we can replace  $R_{+-}$  in Eq. (11) by  $-A_{++} + A_{--}$ , which coincides with the expression given in Ref. [6]. While this expression is obtained in a particular gauge, our formula (11) is gauge-invariant and thus free from the assumption  $\mathbf{d}(k_c) \cdot \mathbf{e}_z \neq 0$ . Note that the integrand (S16) has no physical meaning while the integrated value does. In particular, it diverges as  $\sim (k - k_c)^{-1/2}$  as  $k \rightarrow k_c$ , so that not suitable for numerical evaluation. Let us compare the two formulae,  $\text{Im} \int_{\pi/2}^k dk_2 R_{+-}(k_2)$  and  $\text{Im} \int_{\pi/2}^k dk_2 (-A_{++}(k_2) + A_{--}(k_2))$  with Eq. (S16), with a concrete example. We plot these integrals for the Rice-Mele model Eq. (12) with  $(\delta t, m) = (0.4t, 0.4t)$  in Fig. S1. While the integrals terminated at a generic  $k$  do not coincide, they do at the branching point  $k_c$ .